Acta Oceanol. Sin., 2015, Vol. 34, No. 5, P. 51–59
DOI: 10.1007/s13131-015-0642-7
http://www.hyxb.org.cn
E-mail: hyxbe@263.net

Observed features of temperature, salinity and current in central Chukchi Sea during the summer of 2012

HE Yan[1]*, LIU Na[1], CHEN Hongxia[1], TENG Fei[2], LIN Lina[3], WANG Huiwu[1]

[1] Laboratory of Marine Science and Numerical modeling, The First Institute of Oceanography, State Oceanic Administration, Qingdao 266061, China

[2] College of Oceanography and Environment, Ocean University of China, Qingdao 266100, China

[3] State Key Laboratory of Tropical Oceanography, South China Sea Institute of Oceanology, Chinese Academy of Sciences, Guangzhou 510260, China

Received 12 May 2014; accepted 8 October 2014

Abstract

During the summer of 2012, the fifth CHINARE Arctic Expedition was carried out, and a submersible mooring system was deployed in M5 station located at (69°30.155'N,169°00.654'W) and recovered 50d later. A set of temperature, salinity and current profile records was acquired. The characteristics of these observations are analyzed in this paper. Some main results are achieved as below. (1) Temperature generally decreases while salinity generally increases with increasing depth. The average values of all records are 2.98°C and 32.21 psu. (2) Salinity and temperature are well negatively correlated, and the correlation coefficient between them is –0.84. However, they did not always vary synchronously. Their co-variation featured different characters during different significant periods. (3) The average velocity for the whole water column is 141 mm/s with directional angle of 347.1°. The statistical distribution curve of velocity record number gets narrower with increasing depth. More than 85% of the recorded velocities are northward, and the mean magnitudes of dominated northward velocities are 100–150 mm/s. (4) Rotary spectrum analysis shows that motions with low frequency take a majority of energy in all layers. The most significant energy peaks for all layers are around 0.012 cph (about 3.5 d period), while the tidal motion in mooring area is nonsignificant. (5) Velocities in all layers feature similar and synchronous temporal variations, except for the slight decrease in magnitude and leftward twist from top to bottom. The directions of velocity correspond well to those of surface wind. The average northward volume transport per square meter is 0.1–0.2 m^3/s under southerly wind, but about –0.2 m^3/s during northerly wind burst.

Key words: Chukchi Sea, submersible mooring measurement, 1ong-term observations, temperature and salinity, velocity profile

Citation: He Yan, Liu Na, Chen Hongxia, Teng Fei, Lin Lina, Wang Huiwu. 2015. Observed features of temperature, salinity and current in central Chukchi Sea during the summer of 2012. Acta Oceanologica Sinica, 34(5): 51–59, doi: 10.1007/s13131-015-0642-7

1 Introduction

In the last two decades, the ocean-ice-atmosphere system in the Arctic Ocean undergoes rapid and remarkable changes (Dickson, 1999; Morison et al., 2000), such as air temperature increasing, sea ice reduction, mid-layer water warming and so on. Being an important Arctic marginal sea which is connected to the Pacific through the Bering Strait and directly influenced by Pacific inflow, the Chukchi Sea is very sensitive to global climate behavior. Research on circulations and water masses evolution in the Chukchi Sea benefits clarifying the Polar-Pacific heat transport and the role of Arctic in global climate changes, but is difficult to carry out because of the severe meteorological conditions and seasonal varying ice-cover. Seeing its capability and efficiency in recording long-term hydrological changes consecutively and revealing climatological trend in details, mooring observation is widely employed in scientific research on the Chukchi Sea.

Coachman and Aagaard (1981) evaluated the water transport from a mooring current meter array across the central Chukchi Sea. Weingartner et al. (1998) observed a mean northward flow from a year-long current meter record in Central Channel. Then Weingartner et al. (2005) delineated a circulation sketch with mooring and shipboard observations collected between 1992 and 1995. Pacific inflow with annual mean of about 0.8×10^6 m^3/s (Roach et al., 1995) enters the Arctic Ocean through the Chukchi Sea via the De Long Strait, Herald Valley, Central Channel and Barrow Canyon. Woodgate et al. (2005a) further pointed out based on results from 12 moorings that all these branches are with similar magnitudes (0.1×10^6–0.3×10^6 m^3/s) and significant variations in volume and water properties. They (Woodgate et al., 2005b) also established a monthly climatological dataset from 14 years of moored measurements in the Chukchi Sea, which showed clear interannual variability in temperature and salinity.

Chinese scientists also carried out some mooring observations in the Chukchi Sea and acquired some beneficial results. The characteristics of current in the Bering Strait and the Chuk-

Foundation item: Chinese Polar Environment Comprehensive Investigation and Assessment Programmes, State Oceanic Administration under contract Nos CHINARE2014-03-01 and CHINARE2014-04-03; the Public Science and Technology Research Funds Projects of Ocean under contract No. 201205007-1; the Basic Research Fund under contract No. GY02-2007T08.
*Corresponding author, E-mail: heyan@fio.org.cn

chi Sea were analyzed based on the two current data on the mooring stations during the 2nd Chinese National Arctic Research Expedition (CHINARE) in 2003 (Li et al., 2005). With submersible mooring observations during the third CHINARE in the summer of 2008, main hydrology and current characters were studied (Wang et al., 2011; Chen et al. 2013).

In this paper we analyze the observed features of temperature, salinity and current in central Chukchi Sea with submersible mooring measurements from the fifth CHINARE during the summer of 2012.

2 Data and method

During the 5th CHINARE in summer of 2012, a submersible mooring hydrological observation was carried out in central Chukchi Sea (69°30.155'N,169°00.654'W) from July 21st to September 8th, at Sta. M5 south of Herald Shoal where depth is 53 m (Fig. 1).

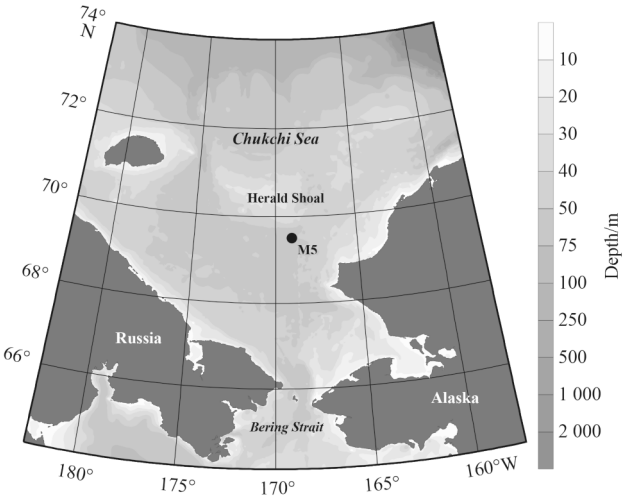

Fig. 1. Location of the mooring system M5.

The mooring system was comprised of a Nortek "aquad" current meter at 14 m depth, an ALEC temperature/depth logger (TD) at 19 m depth, 2 ALEC conductivity/temperature loggers (CT) at 25 and 35 m depths, and 2 conductivity/temperature/depth loggers (CTD) at 18 and 40 mdepths, and at bottom an upward-looking 300 kHz Acoustic Doppler Current Profiler (ADCP) at 41 m depth. An echo blank zone of 4.17 m existing in front of ADCP, the measurements of velocity started from depth of 37 m with 2 m intervals between layers.

All instruments had been corrected and tested before deployment. The instrumental uncertainties of the five temperature sensors are all 0.002°C. The instrumental uncertainties of the four conductivity sensors in top-to-bottom order are 0.003, 0.004, 0.004, and 0.003 mS/cm, respectively. The output salinities of conductivity sensors are in unit of psu. ADCP measurement accuracy of velocity magnitude V is (±0.5%V±0.5) cm/s, while that of velocity direction is ±2°.

The clocks of all instruments had been synchronized before deployment. The sampling intervals of the five temperature/conductivity sensors are set to 15, 30, 30, 30, and 60 s, respectively from top to bottom, while the sampling period of ADCP is set to 20 min with 50 pins in a single period. For the systematic investigation of temperature/salinity profiles, we resampled all temperature/salinity time series and reduced the sampling rates to one datum per minute by moving averaging to make them have identical temporal resolutions. A station observation was achieved in nearby area (69°36.131'N, 168°51.545'W) on September 7th by the same cruise. The temperature/salinity profiles from mooring and station observations were compared and showed good coherence, which proves the reliability of mooring observations from a different perspective.

We compared the ADCP data in the layer of 14 m with "aquad" to test the reliability of velocity dataand found they were well coincided with each other. In the following section only the velocities acquired with ADCP will be used in the analysis of current profiles. When analyzing the temporal variation of velocity profile, velocity data were de-tided through low-pass filtering. Filters to isolate sub-tidal and long period (>40 h) currents were implemented with a 2nd order Butterworth filter.

Thus, we obtained 50-d temperature data in layers of 18, 19, 25, 35 and 40 m, salinity in 18, 25, 35 and 40 m, and velocity data in 17 layers from 5 to 37 m. It is the first time to contain so many measuring instruments in a submersible mooring system for CHINARE.

In addition, wind and precipitation reanalysis data from NCEP/NCAR(http://www.esrl.noaa.gov/psd/data/gridded/data.ncep.reanalysis.html) are also acquired and used in discussionon the variation mechanism of temperature, salinity and velocity.

3 Features of temperature and salinity

3.1 *Temperature*

Time series of temperature measured at depth 18, 19, 25, 35 and 40 m are shown in Fig. 2. The false pulsing signals have been eliminated and a 500-point smoothing was processed to the series to remove some high-frequency information.

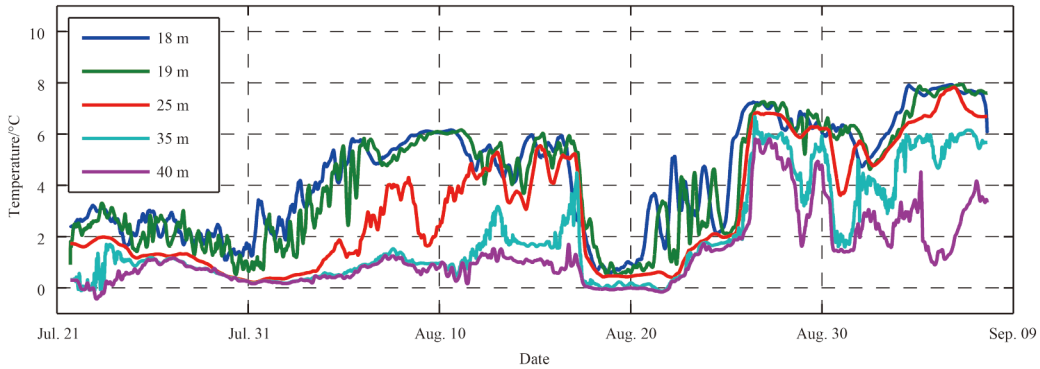

Fig. 2. Temporal variations of temperature in 5 layers.

The average temperatures of the 5 layers are 4.42, 4.18, 3.09, 1.96 and 1.26°C, respectively from top to bottom. The maximum values are 7.93, 7.94, 7.82, 6.68 and 5.82°C, while the minimum values are 0.56, 0.49, 0.22, –0.13 and –0.43°C, respectively. Temperature goes lower with increasing depth in the whole timespan of measurement.

The temporal variation of temperature can be roughly divided into 2 major stages. From the beginning of measurement to August 10th there is a slow heating with some minor fluctuations, while after that temperature of the whole water column fell into drastic oscillations. Both the stages can be divided into some significant periods.

From the beginning of measurement to July 26th, temperatures of the upper layers (18 and 19 m) were fluctuating between 2–3°C, that of mid-layer (25 m) slightly decreased from about 2 to 1°C, while those of the lower layers (35 and 40 m) increased from about 0 to 1°C. During this short period the temperatures of different layers were getting converging and the vertical stratification is weak. This trend sustained till July 31st, and the whole water column was slowly cooling synchronously during these days. In the next stage the upper layer got warmed gradually to 6°C in about 5 d and kept there for another 6 d, while this warming process influenced little on the lower layers. The mid-layer also became warmed but with less strength and more fluctuations. Then from August 11th to 18th there was a cooling process in upper and mid-layers and simultaneously warming process in lower layers, indicating strong vertical mixing induced by surface cooling. The rainfall around mooring area during these days (Fig. 3) may be one reason for this phenomenon. The most dramatic fluctuation occurred during August 18th to 25th. The temperature in upper layers dropped from 6 to 1°C in less than one day. Set aside the fluctuations of upper layers, temperatures of the whole water column kept low around 1–2°C and vertically homogeneous in the following 8 d, and then increased to as high as 6–7°C rapidly. After that, the temperatures fell into strong oscillations with relative low frequency (0.5–1 cycle per day) until the end of measurement. Along with the oscillations, the lower layers turned colder while the upper layers turned slightly warmer.

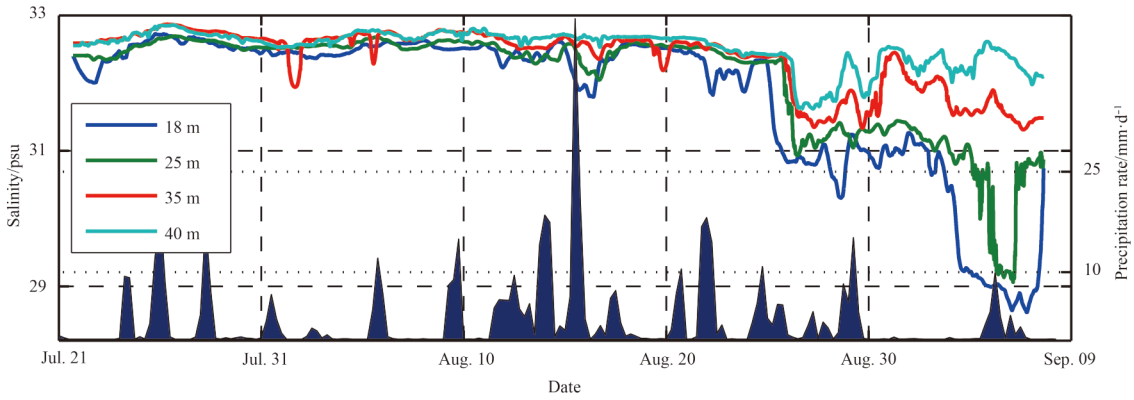

Fig. 3. Temporal variations of salinity in 4 layers.

The temporal variations of temperature in 18 and 19 m layers are similar to each other, while the phase of 19 m layer lags by about 0.5 d, indicating the heat transport direction is downward, both positive and negative. The correlation coefficient between these 2 layers is 0.92, showing strong co-variation. With a correlation coefficient of 0.88, the temporal variations of temperature in 35 and 40 m are also similar to each other, except for that of 35 m layer is obviously higher under a much warmer overlying layer and possibly strong vertical mixing (for example, during August 13–17th and the last few days of measurement). Although the range is much smaller, the variation trend of lower layers is same as that for upper layers during the first of the 2 major stages with a lag of about 2–3 d. However in the second stages, the oscillations of lower layers are much more intensified and become almost synchronous with upper layers. The temporal variation of temperature in 25 m layer shows clear transitional feature between aforementioned 2 modes. It is remarkable that the temperature of mid-layer becomes much closer than before to those of upper layers since August 12th, which indicates strengthened vertical mixing and a deepened upper mixing layer.

3.2 *Salinity*

Time series of salinity measured at depth 18, 25, 35 and 40 m are shown in Fig. 3. The same preprocessing approach has been applied to the salinity series as to temperature.

The average salinities in psu of the 4 layers are 31.83, 32.08, 32.38 and 32.53, respectively from top to bottom. The maximum values are 32.73, 32.69, 32.87 and 32.86, while the minimum values are 28.61, 29.06, 31.31 and 31.62, respectively. Salinityis almost vertically homogeneous before August 12th but goes lower with decreasing depth after that.

The temporal variations of salinity are not so complicated as those of temperature.The whole series can be divided into 3 significant periods. From the beginning of measurement to August 12th, salinity values of the whole water column range in the interval of [31.94, 32.87] with mean value of 32.60. The rainfalls during these days seem not to influence much on the salinity. During August 12th through 25th, salinities of upper (18 m) and middle (25 m) layers underwent notable fluctuations. The falling of salinity seems to be closely related to rainfall events. The salinity variations during August 12th and 17th corresponds to the rainfall event occurred at that period. Following a heavy rainfall on August 16th the salinity at 18 m layer fell down to as low as 31.8 and then recovered after that. Similar case happened during August 21st through 25th.The last period is from August 25th to the end of measurement. During this period the salinity of all layers underwent severe fluctuations and fell down to different extents. Mean values of the 4 layers during this periodlower to

30.27, 30.96, 31.74 and 32.20, respectively from top to bottom. During the first half of this period, salinities in the whole water column fell down, and the fluctuation in 18 m layer is in opposite phase to the other layers. During the second half of this period, salinity in upper and middle layers dramatically fell down to 29 in the last few days and then recovered to 31 by the end of measurement, while the lower layers did not vary much and showed opposite phases. Although there are corresponding rainfall events to the falling of salinity, their intensities are not proportional to the decreasing of salinity, implying a complex dynamics of the variations of salinity.

3.3 *The co-variation between T and S*

During different significant periods the co-variation between temperatures and salinities featured different characters. Although salinity and temperature are well negatively correlated and their correlation coefficients reach –0.71, –0.81, –0.91 and –0.91, respectively in 18, 25, 35 and 40 m layers, they did not always vary synchronously for the whole measuring timespan. In the first 10 d both of them underwent slight rise and fall despite the high-frequency small-range oscillations of temperature in upper layers. However in the next period, salinities of the whole water column remained unchanged and generally uniform while upper and middle layers became much warmer. Then during August 11th through 18th when upper and middle layers were cooling down, the salinities of these layers also decreased simultaneously. A possible explanation is that some cold and fresh water were brought to the sea by heavy rainfalls and spread downward by intensified vertical mixing. Around August 18th when temperatures of all layers suddenly fell down, salinities still remained unchanged. However after that, salinities and temperatures kept varying synchronously but in opposite phases in all layers until the end of measurement.

The complicacy of co-variation between temperature and salinity indicates a complex dynamics. The potential affecting factors include freshwater flux from rainfalls, vertical stirring by surface wind, and horizontal advection by ocean currents, etc. In August, 2012 a huge cyclonic storm centered in the central Arctic moving eastward from Siberia overlaid the mooring area for a long time, which may also increase the complexity of it (Simmonds and Rudeva 2012). Our further research will focus on this issue.

4 Features of ocean current

4.1 *Statistics of current velocity*

We first conduct a statistical study on the magnitudes of velocity in all layers. The average value of velocity for the whole water column is 141 mm/s and in NbW direction (about 347.1°). Summary results of velocity record numbers in different magnitude intervals for each layer are shown in Table 1.

As shown in Table.1, surface layer (Layer 17 in 5 m depth) has the largest velocity magnitude, and the maximum velocity in this layer is 715 mm/s, which is also the maximum value for the whole water column. Along with the increase of water depth, record number in interval [200, 750) also decreases, that in interval [150, 200) increases in upper and middle layers but then decreases in lower layers, while that in interval [0, 150) generally increases.

Table 1. Summary results of record numbers in different magnitude intervals for all layers

Magnitude interval /mm·s^{-1}	Layer (water depth in m)																	Total
	1(37)	2(35)	3(33)	4(31)	5(29)	6(27)	7(25)	8(23)	9(21)	10(19)	11(17)	12(15)	13(13)	14(11)	15(9)	16(7)	17(5)	
[0, 25)	101	68	66	83	113	120	111	126	104	113	119	104	99	87	90	77	72	1552
[25, 50)	323	273	262	250	308	315	299	278	310	295	283	308	263	259	230	205	180	4641
[50, 75)	636	576	495	505	442	410	408	393	363	363	404	399	405	376	359	288	266	7088
[75, 100)	692	557	579	526	489	456	435	422	428	430	381	410	453	419	412	378	335	7802
[100, 150)	1077	962	939	919	930	951	971	928	889	875	863	842	789	827	770	710	687	14929
[150, 200)	432	616	653	684	690	718	711	755	751	734	747	693	693	643	585	576	564	11245
[200, 250)	144	288	328	349	347	338	336	347	393	365	347	347	354	391	410	407	428	5919
[250, 500)	94	159	177	183	180	191	228	250	261	324	355	396	443	495	631	837	914	6118
[500, 750)	0	0	0	0	0	0	0	0	0	0	0	0	0	2	12	21	53	88

For the whole water column the magnitude interval [100, 200) is a “peak area” in statistical distribution curve of record number, which contains more than 40% of the records. However, in different layers the distribution curves show different features. As seen in Table 1 and Fig. 4, the velocity range in upper layers (5m as representative) is much wider than those in middle (21 m) and lower (37 m) layers. The numbers of velocity record those greater than 250 mm/s decrease rapidly with depth increasing. The velocity records in 21 m layer are mostly concentrated in 100–200 mm/s band, and those of 37 m layer almost fall in a narrow band between 50 and 150 mm/s. The average value in 5 m layer is 191

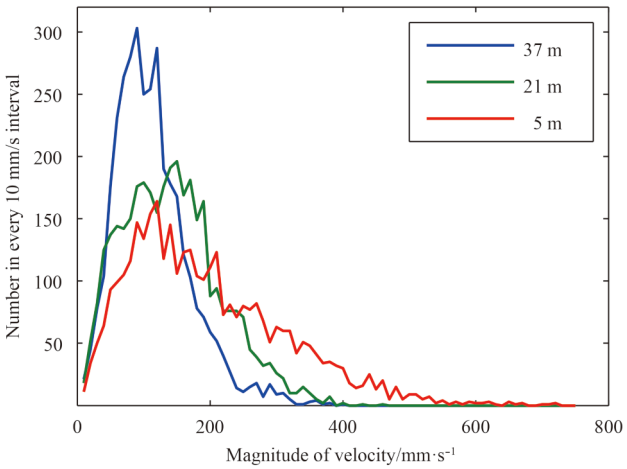

Fig. 4. Distribution curves of record number in several representative layers.

mm/s, but only 137 mm/s in 21 m layer and 108 mm/s in 37 m layer. It should be mentioned that the instrumental error is not eligible whereas the velocity magnitudes are small. For typical 100 and 150 mm/s velocities the maximum relative errors may reach 5.5% and 3.8%, respectively.

A statistical summary on velocity characters in different directions has been also carried out. Figure 5 shows the probability distribution of velocity records in every 18° interval and their mean values in these intervals. We can see that more than 85% of the recorded velocities are northward, among which about 50% are located in the 60° angle area centered at due north. The recorded velocities pointing to southwest directions have largest mean magnitudes that over 150 mm/s though the numbers of them are small. Few records pointing to southeast and their velocity magnitudes are also the smallest. The mean magnitudes of dominated northward velocities are 100–150 mm/s, which is an important feature of the flow field in mooring area.

4.2 *Spectral analysis of current*

In order to reveal the temporal varying characteristics of current, the rotary spectra analysis was also carried out folloing the method provided by Gonella (1972). The anticlockwise spectrum $S_+(f)$ and clockwise spectrum $S_-(f)$ give the energy distributions of vector that rotates anticlockwisely and clockwisely, respectively in frequency f. The total spectrum S_T gives the total energy distribution with frequency. The rotary coefficient C_r represents the rotary property of vector. When C_r=–1 or 1, the flow becomes pure curcular motion, anticlockwise or clockwise; when C_r=0, the flow is reciprocating motion.

Figure 6 shows the features of S_T for 3 representative layers.

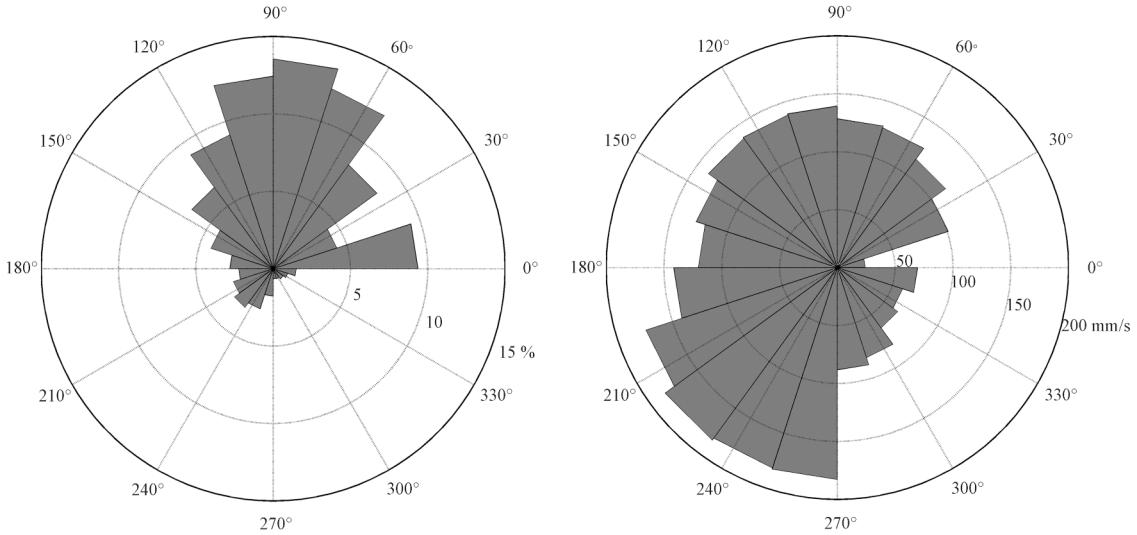

Fig. 5. Probability distribution of velocity records by directions (left), and their mean values (right).

The additional window in lower left corner zooms in the high frequency portion of the curves. The curve sections with frequency lower than 10^{-3} are not discussed here since they represent variations with period longer than the timespan of measurement. A remarkability test was processed to each spectrum, and the breaklines in Fig. 6 show the threshold values to distinguish real spectral peaks from red noises on 95% confidence interval. We can see that motions with low frequency take a majority of energy in all layers. Energy density for upper layer is higher than that for lower layer, which corresponds to the result of statistical study. The most significant energy peaks for all layers are around 0.012 cph, indicating a strong variation with about 3.5 d period, which is the only ones that are considered as remarkable spectral peaks but not red noises on 95% confidence interval. In tidal frequency area, there are only weak peaks around 0.07–0.08 cph in upper and mid-layers, which represent variations in M2 and local inertial frequency, while in lower layer this variation does not exist, and another 2 weak peaks around 0.6 and 0.9 cph appear instead. Although the spectral characters of movements in tidal frequency area are also discussed here, their energy densities are about 2–3 order of magnitude lower than those in low frequency area, which means that the tidal motion in mooring area is nonsignificant. Remarkability test indicate that tidal frequency

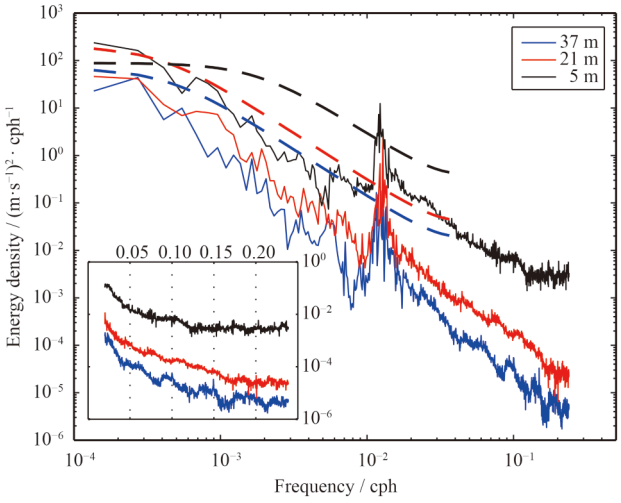

Fig. 6. Total spectrum S_T for the 3 representative layers.

movements are potentially red noises. The results of harmonic analysis also shows that the tidal movements take only five percents of total kinetic energy. This conclusion is in accord with previous work (Woodgate et al., 2005a).

Figures 7–10 show the features of S_-, S_+ and rotary coefficients in 3 representative layers and the corresponding threshold breaklines for 95% confidence intervals. In 5 m layer the flow vector features notable rotating property except for the section of 0.005–0.015 cph. The variation with higher frequency are anticlockwise while that with lower frequency are clockwise. Curve of C_T shows that in 0.02–0.1 cph interval (0.4–2 d period) the current in this layer is almost cycling anticlockwisely. In 21 m layer the variation has similar but weaker rotating property as that in 5 m layer. In 37 m layer both the distributions of energy density and rotary coefficient show that the rotating is very weak in high frequency section but of similar features as overlaying layers in low frequency section.

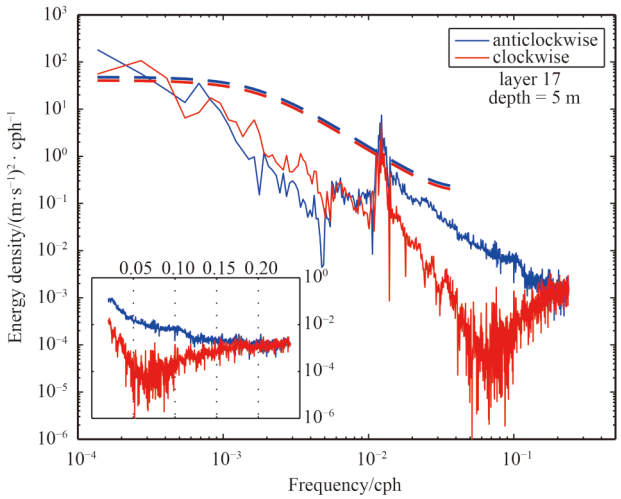

Fig. 7. S_- and S_+ for layer 17 (5 m depth).

4.3 *Current profile features*

Figure 11 displays the temporal variations of velocity in each observed layer. A lowpass filtering has been processed in advance to remove the insignificant high frequency signals.

Velocities in all layers feature similar and synchronous variations, except for the slight decrease in magnitude and leftward twist from top to bottom. The temporal variation can also be divided into several significant periods like temperature and salinity. On the first 3 d the velocities of all layers were small and the flow directions of lower and surface layers are almost opposite. Then the velocities in all layers turned northward and maintained 0.1–0.2 m/s magnitudes for the next 15 d. After that since August 8th the flow became intermittent but still generally northward. However in the last 8 d of measurement, the flow turned southward dramatically, southwestward in upper layers and south-southwestward in lower layer, and recovered northward again in the last 2 d.

The variation of flow appears to be related to the variation of surface wind. Figure 12 shows daily surface wind vector in the mooring area. The directions of velocity correspond well to those of wind, especially in the second half of the timespan. The current went northward when wind blew northward, while when wind turned southward the current rotated too. However, because of the existence of the huge cyclonic storm, current may be influenced more by the wind system over the entire region than by local wind force. This issue needs further concern and more systematic study.

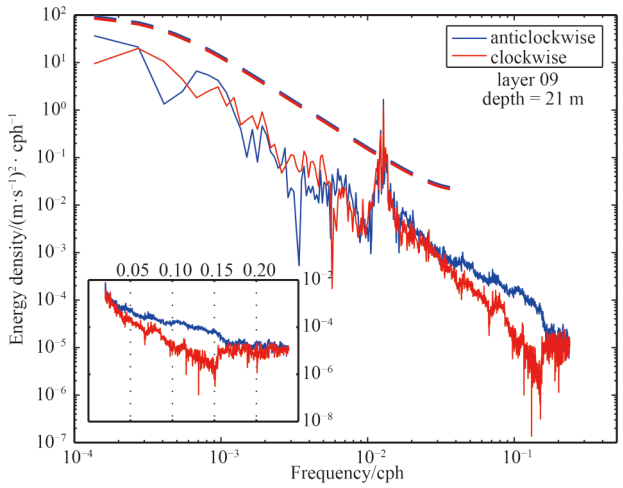

Fig. 8. S_- and S_+ for layer 9 (21 m depth).

Since meridional flows are dominated during the measurement timespan, northward volume transport per square meter is calculated to evaluate the water transport capacity in the mooring area. The mooring system was located at the southern entrance of the Central Channel, which is on the pathway of northward flowing Bering Shelf Water (Weingartner et al., 2005). During summer, this area is dominated by southwesterly wind, and the Bering Shelf Water flows northward under the control of topography and wind forcing. The flow characters during the first half timespan of measurement agree with this situation, so we take the mean northward transport per square meter of 0.1–0.2 m^3/s as a guess value the typical transport of Bering Shelf Water.

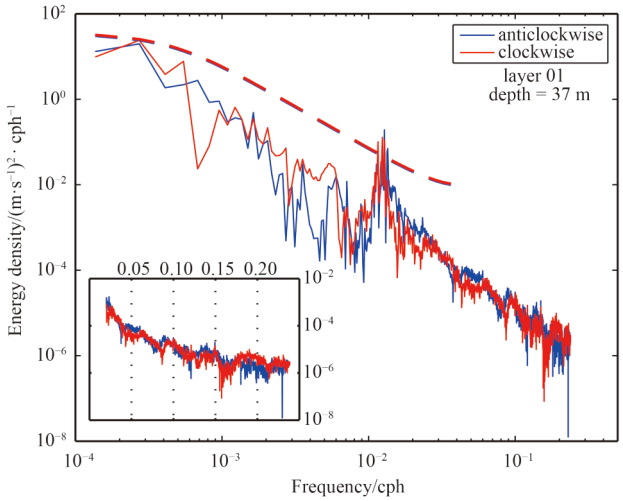

Fig. 9. S_- and S_+ for layer 1 (37 m depth).

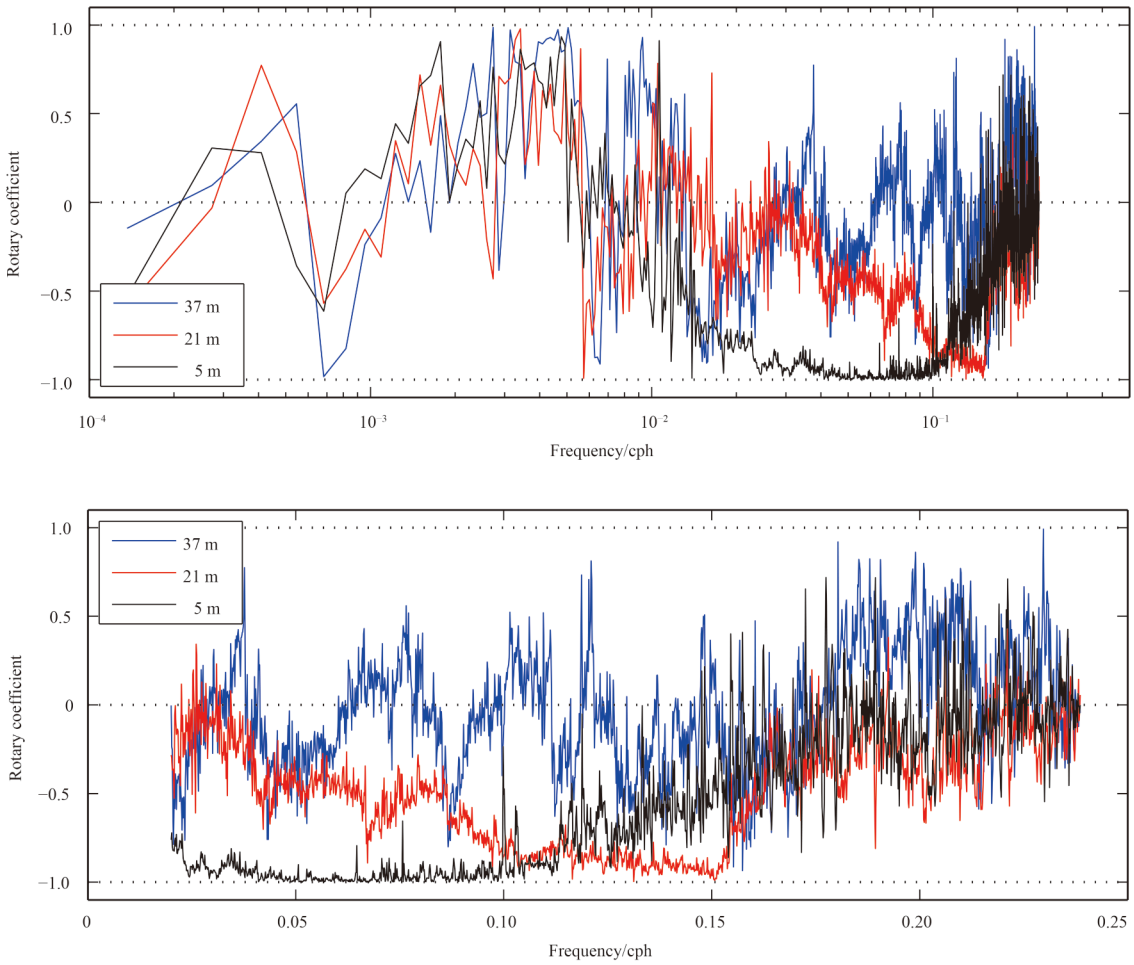

Fig. 10. Rotary coefficients C_r for the 3 representative layers (top), and the detailed view for high frequency potion (bottom).

5 Conclusions

According to the above analysis results, some conclusions are reached for the mooring area during 2012 summer:

(1) Temperature generally decreases with increasing depth. The average values of the 5 layers are 4.42, 4.18, 3.09, 1.96 and 1.26°C, respectively from top to bottom. The maximum value is 7.94°C while the minimum value is –0.43°C during the measurement.

Salinity generally increases with increasing depth. The average values in unit psu of the 4 layers are 31.83, 32.08, 32.38 and 32.53, respectively from top to bottom. The maximum value is 32.87 while the minimum value is 28.61 during the measurement.

(2) Salinity and temperature are well negatively correlated. Their correlation coefficients are –0.71, –0.81, –0.91 and –0.91, respectively in 18, 25, 35 and 40 m layers. However, they did not always vary synchronously. Their co-variation featured different characters during different significant periods. It seems that rainfalls can influence the vertical distributions of temperature and salinity, especially in upper layers.

(3) The average velocity for the whole water column is 141 mm/s with directional angle of 347.1°. The maximum velocity is 715 mm/s, which is measured in 5 m layer. The average value in 5 m layer is 191 mm/s, but only 137 mm/s in 21 m layer and 108 mm/s in 37 m layer. The peak of statistical distribution curve of velocity record number for the whole water column is located in the magnitude interval [100, 200), while the curve for single layer becomes narrower with depth increasing.

A statistical summary on velocity characters in different directions has been also carried out. More than 85% of the recorded velocities are northward, among which about 50% are located in the 60° angle area centered at due north. The mean magnitudes of dominated northward velocities are 100–150 mm/s.

(4) Rotary spectrum analysis shows that motions with low frequency take a majority of energy in all layers. The most significant energy peaks for all layers are around 0.012 cph (about 3.5 d period). Energy densities in tidal frequency area are about 2–3 order of magnitude lower than those in low frequency area, which means that the tidal motion in mooring area is nonsignificant.

(5) Velocities in all layers feature similar and synchronous variations, except for the slight decrease in magnitude and leftward twist from top to bottom. The variation of flow appears to be related to the variation of surface wind. The directions of velocity correspond well to those of wind. The average northward volume transport is 0.1–0.2 m^3/s per square meter under southerly wind, but about –0.2 m^3/s during northerly wind burst.

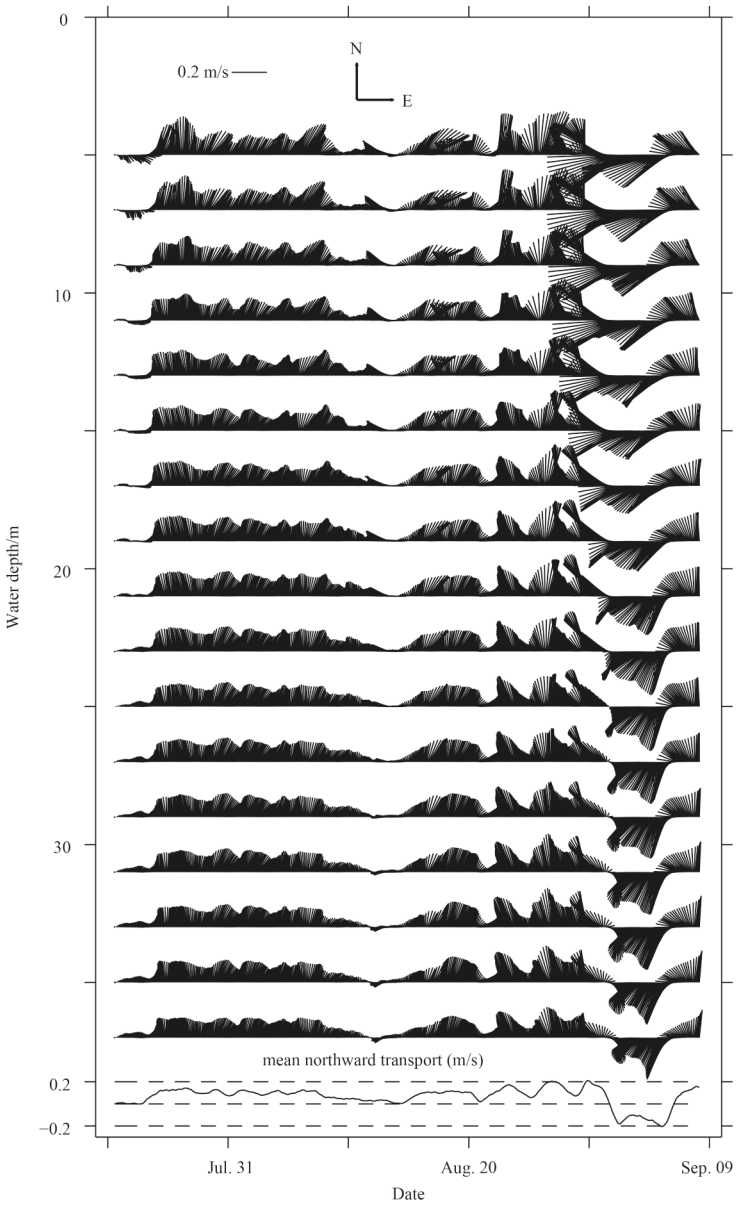

Fig. 11. Temporal variations of velocity in all layers.

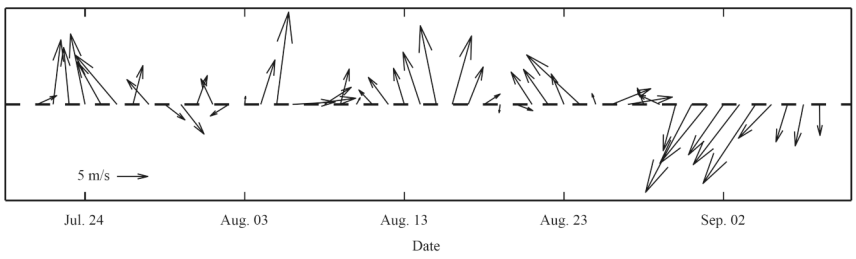

Fig. 12. Daily surface wind vector in the mooring area.

Acknowledgements

We thank the crew of research vessel *Xuelong* in the 5th CHINARE and those who help with the mooring system design.

References

Chen Hongxia, Wang Huiwu, Shu Qi, et al. 2013. Ocean current observation and spectrum analysis in central Chukchi Sea during the summer of 2008. Acta Oceanologica Sinica, 32(3): 10–18

Coachman L K, Aagaard K. 1981. Re-evaluation of water transports in the vicinity of Bering Strait. In: Hood D W, Calder J A, eds. The Eastern Bering Sea Shelf: Oceanography and Resources, Vol. 1. Washington, D C: National Oceanic and Atmospheric Administration, 95–110

Dickson B. 1999. Oceanography: All change in the Arctic. Nature, 397(6718): 389–391

Gonella J. 1972. A rotary-component method for analysing meteorological and oceanographic vector time series. Deep Sea Research and Oceanographic Abstracts, 19(12): 833–846

Li Lei, Du Ling, Zhao Jinping, et al. 2005. The fundamental characteristics of current in the Bering Strait and the Chukchi Sea from July to September 2003. Acta Oceanologica Sinica, 24(6): 1–11

Morison J, Aagaard K, Steele M. 2000. Recent environmental changes in the Arctic: a review. Arctic, 53(4): 359–371

Roach T A, Aagaard K, Pease H C, et al. 1995. Direct measurements of transport and water properties through the Bering Strait. Journal of Geophysical Research: Oceans (1978–2012), 100(C9): 18443–18457

Simmonds I, Rudeva I. 2012. The great Arctic cyclone of August 2012. Geophysical Research Letters, 39(23): L23709, doi: 10.1029/2012GL054259

Wang Huiwu, Chen Hongxia, Lü Liangang, et al. 2011. Study of tide and residual current observations in Chukchi Sea in the summer 2008. Haiyang Xuebao (in Chinese), 33(6): 1–8

Weingartner T, Aagaard K, Woodgate R, et al. 2005. Circulation on the north central Chukchi Sea shelf. Deep-Sea Research Part II: Topical Studies in Oceanography, 52(24–26): 3150–3174

Weingartner T, Cavalieri D J, Aagaard K, et al. 1998. Circulation, dense water formation, and outflow on the northeast Chukchi shelf. Journal of Geophysical Research: Oceans (1978–2012), 103(C4): 7647–7661

Woodgate R A, Aagaard K, Weingartner T J. 2005a. A year in the physical oceanography of the Chukchi Sea: Moored measurements from autumn 1990–1991. Deep-Sea Research Part II: Topical Studies in Oceanography, 52(24–26): 3116–3149

Woodgate R A, Aagaard K, Weingartner T J. 2005b. Monthly temperature, salinity, and transport variability of the Bering Strait through flow. Geophysical Research Letters, 32(4): 1–4